

# Relative intensity squeezing by four-wave mixing with loss: an analytic model and experimental diagnostic

M. Jasperse,<sup>1,2,\*</sup> L. D. Turner,<sup>2</sup> and R. E. Scholten<sup>1</sup>

<sup>1</sup>ARC Centre of Excellence for Coherent X-Ray Science, University of Melbourne,  
VIC 3010, Australia

<sup>2</sup>School of Physics, Monash University, VIC 3800, Australia

[\\*martijn.jasperse@monash.edu](mailto:martijn.jasperse@monash.edu)

**Abstract:** Four-wave mixing near resonance in an atomic vapor can produce relative intensity squeezed light suitable for precision measurements beyond the shot-noise limit. We develop an analytic distributed gain/loss model to describe the competition of mixing and absorption through the non-linear medium. Using a novel matrix calculus, we present closed-form expressions for the degree of relative intensity squeezing produced by this system. We use these theoretical results to analyze experimentally measured squeezing from a <sup>85</sup>Rb vapor and demonstrate the analytic model's utility as an experimental diagnostic.

© 2018 Optical Society of America

**OCIS codes:** (190.4380) Nonlinear optics, four-wave mixing; (270.6570) Squeezed states.

---

## References and links

1. C. F. McCormick, V. Boyer, E. Arimondo, and P. D. Lett, "Strong relative intensity squeezing by four-wave mixing in rubidium vapor," *Opt. Lett.* **32**, 178–180 (2007).
  2. Q. Glorieux, L. Guidoni, S. Guibal, J.-P. Likforman, and T. Coudreau, "Strong quantum correlations in four wave mixing in <sup>85</sup>Rb vapor," (SPIE, 2010), vol. 7727 of *Proc. SPIE*, p. 772703.
  3. C. F. McCormick, A. M. Marino, V. Boyer, and P. D. Lett, "Strong low-frequency quantum correlations from a four-wave-mixing amplifier," *Phys. Rev. A* **78**, 043816 (2008).
  4. V. Boyer, A. M. Marino, and P. D. Lett, "Generation of spatially broadband twin beams for quantum imaging," *Phys. Rev. Lett.* **100**, 143601 (2008).
  5. V. Boyer, A. M. Marino, R. C. Pooser, and P. D. Lett, "Entangled images from four-wave mixing," *Science* **321**, 544–547 (2008).
  6. V. Boyer, C. F. McCormick, E. Arimondo, and P. D. Lett, "Ultraslow propagation of matched pulses by four-wave mixing in an atomic vapor," *Phys. Rev. Lett.* **99**, 143601 (2007).
  7. R. C. Pooser, A. M. Marino, V. Boyer, K. M. Jones, and P. D. Lett, "Low-noise amplification of a continuous-variable quantum state," *Phys. Rev. Lett.* **103**, 010501 (2009).
  8. Q. Glorieux, R. Dubessy, S. Guibal, L. Guidoni, J.-P. Likforman, T. Coudreau, and E. Arimondo, "Double- $\Lambda$  microscopic model for entangled light generation by four-wave mixing," *Phys. Rev. A* **82**, 033819 (2010).
  9. C. C. Gerry and P. L. Knight, *Introductory Quantum Optics*, (Cambridge University Press, 2005).
  10. H. A. Bachor and T. C. Ralph, *A Guide to Experiments in Quantum Optics*, (Wiley-VCH Verlag, 2004).
  11. C. M. Caves, "Quantum-mechanical radiation-pressure fluctuations in an interferometer," *Phys. Rev. Lett.* **45**, 75–79 (1980).
  12. R. Loudon, *The Quantum Theory of Light* (Oxford University Press, 1983), 2nd ed.
  13. R. Loudon, "Theory of noise accumulation in linear optical-amplifier chains," *IEEE J. Quantum Electron.* **21**, 766–773 (1985).
  14. C. M. Caves and D. D. Crouch, "Quantum wideband traveling-wave analysis of a degenerate parametric amplifier," *J. Opt. Soc. Am. B* **4**, 1535–1545 (1987).
-

## 1. Introduction

Relative intensity squeezing by four-wave mixing in an atomic vapor is emerging as a promising technique for performing high-precision measurements beyond the shot-noise limit. First demonstrated by McCormick et al. [1], the technique uses atomic coherences to produce quantum correlated “twin beams”, enabling the shot-noise of one beam to be measured and subtracted from the other to obtain a low-noise differential measurement; for example of a weakly absorbing sample. This scheme was recently shown to reduce the relative intensity noise by  $9.2 \pm 0.5$  dB below the shot-noise limit [2], and noise reduction has been observed in both the low Fourier frequency [3] and multi-mode imaging [4, 5] domains.

Furthermore, as one of the twin beams is near-resonant with the atoms, this squeezing technique has promising applications in quantum information processing [6, 7]. However, absorption near resonance degrades the quantum correlations. Both mixing gain and absorption losses occur simultaneously as the beams propagate through the vapor, and are therefore competing processes.

Earlier theoretical investigations of this system have applied numerical methods [3] and the Heisenberg-Langevin formalism [8] to predict the resulting degree of squeezing. The numerical model demonstrated excellent agreement with experimental results, but it can be difficult to gain insight into the competing processes from numerical calculations. The Heisenberg-Langevin model provided a microscopic description of a specific four-wave mixing configuration in a cold atomic gas, which accurately predicted the resulting gain profiles. However, calculation of the predicted squeezing required complex matrix integrals and no comparison to experimentally measured squeezing was presented.

In this work, we present a very general approach for determining the squeezing produced by a four-wave mixing system, and develop a matrix-based analysis method to include arbitrarily many injected vacuum modes. Considering special cases, simple closed-form expressions are easily obtained. Finally, we present experimentally measured squeezing from four-wave mixing in a rubidium-85 vapor, and demonstrate how the model can be used as a diagnostic tool to determine the limiting technical factors.

## 2. Relative intensity squeezing

The “double- $\Lambda$ ” four-wave mixing scheme introduced by McCormick et al [1] uses a high-intensity “pump” beam to drive a cycle of four off-resonant transitions in a hot rubidium vapor, causing the emission of correlated “probe” and “conjugate” photons (Fig. 1A). The probe transition is stimulated by a seed laser incident at an angle  $\theta$  to the pump, resulting in the spontaneous emission of the conjugate on the opposite side of the pump beam (Fig. 1B). The beam powers are measured individually and subtracted to obtain the relative intensity noise as measured on a spectrum analyzer (S.A.).

Labelling the Fock-space annihilation operators of the probe, conjugate and pump by  $\hat{a}$ ,  $\hat{b}$  and  $\hat{c}$  respectively and the interaction strength by  $\xi$ , the interaction picture Hamiltonian is

$$\mathcal{H}_i = i\hbar(\xi \hat{b}^\dagger \hat{c} \hat{a}^\dagger \hat{c} - \xi^* \hat{c}^\dagger \hat{a} \hat{c}^\dagger \hat{b}).$$

In the “undepleted pump” approximation, the intense pump beam remains in its initial coherent state  $|\psi_c\rangle$  and the substitution  $\hat{c} \rightarrow \psi_c$  can be made:

$$\mathcal{H}_i = i\hbar(\xi \psi_c^2 \hat{b}^\dagger \hat{a}^\dagger - \xi^* (\psi_c^*)^2 \hat{a} \hat{b}).$$

The time-evolution of this Hamiltonian over the interaction time-scale  $\tau$  is

$$\hat{S} \equiv \exp(-i\mathcal{H}_i\tau/\hbar) = \exp(s\hat{b}^\dagger \hat{a}^\dagger - s^* \hat{a} \hat{b}), \quad \text{where } s = \xi \psi_c^2 \tau. \quad (1)$$

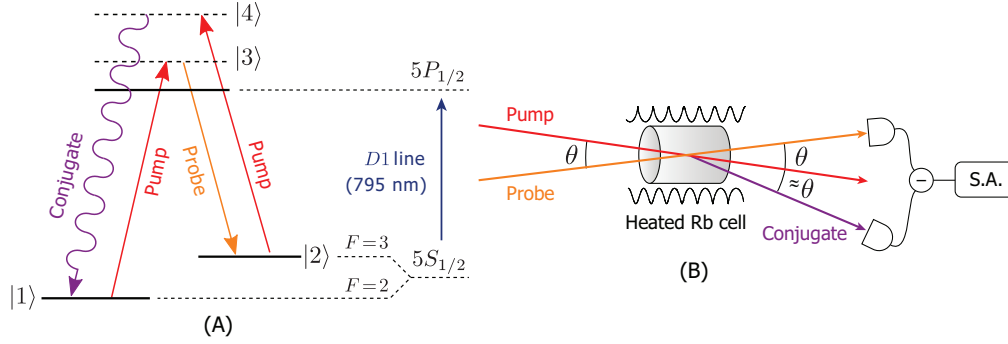


Fig. 1. (A) Four-wave mixing energy-level transitions and (B) experimental schematic.

This is the two-mode squeezing operator for modes  $\hat{a}$  and  $\hat{b}$ , where  $s$  is the “squeezing parameter” [9]. The four-wave mixing system therefore produces a two-mode squeezed state, reducing amplitude difference noise at the expense of increasing phase difference noise [5].

The phase of  $s$  results in a rotation of the (arbitrary) measurement quadratures, so  $s$  may be taken as real and positive. The probe and conjugate modes  $\hat{a}$  and  $\hat{b}$  are then transformed as

$$\hat{a} \rightarrow \hat{S}^\dagger \hat{a} \hat{S} = \cosh(s)\hat{a} + \sinh(s)\hat{b}^\dagger \quad \text{and} \quad \hat{b}^\dagger \rightarrow \hat{S}^\dagger \hat{b}^\dagger \hat{S} = \sinh(s)\hat{a} + \cosh(s)\hat{b}^\dagger. \quad (2)$$

Defining the number operator of the incident probe beam as  $\hat{N}_0 \equiv \hat{a}_0^\dagger \hat{a}_0$  and making the bright beam approximation  $\langle \hat{N}_0 \rangle \gg 1$ , the number operators after squeezing become

$$\langle \hat{N}_a \rangle \equiv \langle \hat{a}^\dagger \hat{a} \rangle \simeq G \langle \hat{N}_0 \rangle \quad \text{and} \quad \langle \hat{N}_b \rangle \equiv \langle \hat{b}^\dagger \hat{b} \rangle \simeq (G-1) \langle \hat{N}_0 \rangle,$$

where  $G \equiv \cosh^2 s$  is the increase in probe intensity, termed the “mixing gain”.

The relative intensity operator  $\hat{N}_a - \hat{N}_b$  is unchanged by  $\hat{S}$ , so  $\text{Var}(\hat{N}_a - \hat{N}_b) = \text{Var}(\hat{N}_0)$ . Hence the beams have been amplified without increasing the relative intensity noise; they are relative intensity squeezed. The noise figure of the process (or “degree of squeezing”) is the ratio of the measured noise to the corresponding shot-noise level for equal optical power. Assuming an initially shot-noise limited probe, the noise figure is

$$\text{NF} \equiv \frac{\text{Var}(\hat{N}_a - \hat{N}_b)}{\langle \hat{N}_a \rangle + \langle \hat{N}_b \rangle} = \frac{\langle \hat{N}_0 \rangle}{G \langle \hat{N}_0 \rangle + (G-1) \langle \hat{N}_0 \rangle} = \frac{1}{2G-1}. \quad (3)$$

Therefore the measured noise power can be reduced arbitrarily below the shot-noise limit in the limit of ideal detection. However, optical losses are unavoidable and occur both within the medium (e.g. absorption) and after it (e.g. imperfect detection). These losses randomly eject photons from the probe and conjugate beams, decorrelating their intensities and degrading the observed degree of squeezing. We now construct models to quantify this effect.

### 3. Optical losses after squeezing

We initially consider only losses that occur after mixing, such as from imperfect optical transmission or detection efficiency. These losses are modelled by a beamsplitter with an empty port [10] whose output state is a combination of the input and vacuum modes, contributing “vacuum fluctuations” to the transmitted beam [11]. Denoting the vacuum modes introduced by losses on the probe and conjugate by the annihilation operators  $\hat{x}$  and  $\hat{y}$  respectively, the standard beam-splitter input-output relations [12] give

$$\hat{a} \rightarrow \sqrt{\eta_a} \hat{a} + \sqrt{1-\eta_a} \hat{x} \quad \text{and} \quad \hat{b} \rightarrow \sqrt{\eta_b} \hat{b} + \sqrt{1-\eta_b} \hat{y}, \quad (4)$$

where  $\eta_a$  and  $\eta_b$  are the fractions of the probe and conjugate intensities transmitted. The relative intensity noise can then be expressed in terms of the individual beam variances and covariance to give

$$\text{Var}(\hat{N}_a - \hat{N}_b) = \eta_a^2 \text{Var}(\hat{N}_a) + \eta_a(1 - \eta_a)\langle \hat{N}_a \rangle + \eta_b^2 \text{Var}(\hat{N}_b) + \eta_b(1 - \eta_b)\langle \hat{N}_b \rangle - 2\eta_a\eta_b \text{CoVar}(\hat{N}_a, \hat{N}_b).$$

Computing the variances using Eq. (2), the noise figure corresponding to four-wave mixing followed by optical losses is

$$\text{NF} = 1 + \frac{2(G-1)(G(\eta_a - \eta_b)^2 - \eta_b^2)}{G\eta_a + (G-1)\eta_b}. \quad (5)$$

This expression highlights the importance of balanced beam detection, as unbalanced losses ( $\eta_a \neq \eta_b$ ) result in detection of amplified noise instead of squeezing.

#### 4. Optical losses during squeezing: Interleaved gain/loss model

The four-wave mixing process consists of Raman transitions between the hyperfine ground states (Fig. 1A), which are most efficient when the intermediate virtual level is tuned close to resonance. However, this also increases direct absorption from the Doppler broadened transition, increasing losses and reducing correlations. To analyze this trade-off, we develop a model for the effect of competing mixing and absorption on relative intensity squeezing.

Following the approach of the numerical model presented in Ref. [3], the beam trajectories through the medium are divided into  $N$  discrete interleaved stages of gain and loss (Fig. 2). Distributed models of this type were first proposed by Loudon [13], and applied by Caves and Crouch [14] to model distributed squeezing losses in a single-mode parametric amplifier. We present a fully analytical model of the relative squeezing produced by this system in the continuum limit, including losses on both beams.

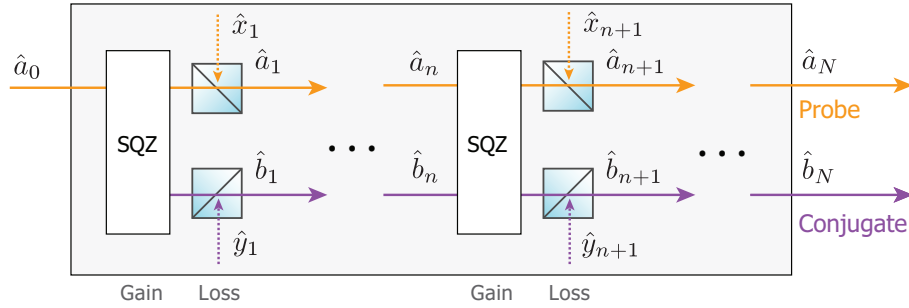


Fig. 2. Competing gain and loss processes modelled by interleaved stages of squeezing (SQZ) and loss.

Each stage comprises ideal squeezing (by parameter  $s$ ) followed by loss (represented by transmission coefficients  $t_a$  on the probe and  $t_b$  on the conjugate). Consecutive stages of the model are related by combining Eq. (2) with Eq. (4) to give

$$\begin{aligned} \hat{a}_{n+1} &= t_a(\cosh s \hat{a}_n + \sinh s \hat{b}_n^\dagger) + \sqrt{1 - t_a^2} \hat{x}_{n+1}, \\ \hat{b}_{n+1}^\dagger &= t_b(\sinh s \hat{a}_n + \cosh s \hat{b}_n^\dagger) + \sqrt{1 - t_b^2} \hat{y}_{n+1}^\dagger. \end{aligned} \quad (6)$$

The overall model is parameterized in terms of the overall squeezing parameter  $S$  in the absence of losses, and transmissions  $T_a$  and  $T_b$  in the absence of squeezing. These are related to the incremental coefficients above by  $s = S/N$ ,  $t_a = T_a^{1/2N}$  and  $t_b = T_b^{1/2N}$ .

This transformation can be written in matrix form and applied recursively to express the output beam operators  $\hat{a}_N$  and  $\hat{b}_N^\dagger$  as a sum of the incident beam operators ( $\hat{a}_0$  and  $\hat{b}_0^\dagger$ ) and the injected vacuum operators ( $\hat{x}_i$  and  $\hat{y}_i^\dagger$ ) as

$$\begin{aligned} \begin{pmatrix} \hat{a}_N \\ \hat{b}_N^\dagger \end{pmatrix} &= \mathbf{A} \begin{pmatrix} \hat{a}_{N-1} \\ \hat{b}_{N-1}^\dagger \end{pmatrix} + \begin{pmatrix} \sqrt{1-t_a^2} \hat{x}_N \\ \sqrt{1-t_b^2} \hat{y}_N^\dagger \end{pmatrix} \\ &= \mathbf{A}^N \begin{pmatrix} \hat{a}_0 \\ \hat{b}_0^\dagger \end{pmatrix} + \sum_{i=1}^N \mathbf{A}^{N-i} \begin{pmatrix} \sqrt{1-t_a^2} \hat{x}_i \\ \sqrt{1-t_b^2} \hat{y}_i^\dagger \end{pmatrix}, \end{aligned} \quad (7)$$

where

$$\mathbf{A} = \begin{pmatrix} t_a \cosh s & t_a \sinh s \\ t_b \sinh s & t_b \cosh s \end{pmatrix}. \quad (8)$$

For algebraic simplicity, we introduce a polymorphic operator  $\hat{z}_i$  consisting of the probe annihilation and conjugate creation operators  $\hat{z}_1 = \hat{a}_0$  and  $\hat{z}_2 = \hat{b}_0^\dagger$ , followed by the injected vacuum operators  $\hat{z}_{2i+1} = \hat{x}_i$  and  $\hat{z}_{2i+2} = \hat{y}_i^\dagger$  for  $1 \leq i \leq N$ . Expanding Eq. (7) in terms of this operator and a set of coefficients  $\alpha_i$  and  $\beta_i$  gives

$$\begin{aligned} \hat{a}_N &= \alpha_1 \hat{a}_0 + \alpha_2 \hat{b}_0^\dagger + \alpha_3 \hat{x}_1 + \alpha_4 \hat{y}_1^\dagger + \cdots + \alpha_{2N+1} \hat{x}_N + \alpha_{2N+2} \hat{y}_N^\dagger = \sum_i \alpha_i \hat{z}_i, \\ \hat{b}_N^\dagger &= \beta_1 \hat{a}_0 + \beta_2 \hat{b}_0^\dagger + \beta_3 \hat{x}_1 + \beta_4 \hat{y}_1^\dagger + \cdots + \beta_{2N+1} \hat{x}_N + \beta_{2N+2} \hat{y}_N^\dagger = \sum_i \beta_i \hat{z}_i. \end{aligned} \quad (9)$$

Using standard statistical identities, the relative intensity operator and its variance are

$$\begin{aligned} \hat{N}_a - \hat{N}_b &= \hat{a}_N^\dagger \hat{a}_N - \hat{b}_N^\dagger \hat{b}_N = \sum_{i,j} (\alpha_i \alpha_j - \beta_i \beta_j) \hat{z}_i^\dagger \hat{z}_j + 1 \quad \text{and} \\ \text{Var}(\hat{N}_a - \hat{N}_b) &= \sum_{i,j,k,l} (\alpha_i \alpha_j - \beta_i \beta_j) (\alpha_k \alpha_l - \beta_k \beta_l) \text{CoVar}(\hat{z}_i^\dagger \hat{z}_j, \hat{z}_k^\dagger \hat{z}_l). \end{aligned}$$

In the bright probe beam approximation ( $\hat{N}_0 \gg 1$ ), this variance simplifies to

$$\text{Var}(\hat{N}_a - \hat{N}_b) = (\alpha_1^2 - \beta_1^2)^2 \text{Var}(\hat{N}_0) + \sum_{i>1} (\alpha_1 \alpha_i - \beta_1 \beta_i)^2 \langle \hat{N}_0 \rangle.$$

The shot-noise limit is  $\langle \hat{N}_a + \hat{N}_b \rangle = (\alpha_1^2 + \beta_1^2) \langle \hat{N}_0 \rangle$ , so the degree of squeezing for an initially shot-noise limited probe with  $\text{Var}(\hat{N}_0) = \langle \hat{N}_0 \rangle$  is

$$\text{NF} \equiv \frac{\text{Var}(\hat{N}_a - \hat{N}_b)}{\langle \hat{N}_a + \hat{N}_b \rangle} = \frac{\sum_{i=1}^N (\alpha_1 \alpha_i - \beta_1 \beta_i)^2}{\alpha_1^2 + \beta_1^2}. \quad (10)$$

It remains to express the  $\alpha_i$ ,  $\beta_i$  coefficients in terms of the model parameters  $T_a$ ,  $T_b$  and  $S$ , and hence obtain an ab-initio expression for the degree of squeezing.

Equating the coefficients of Eq. (7) and Eq. (9) leads to

$$\begin{pmatrix} \alpha_1 & \alpha_2 \\ \beta_1 & \beta_2 \end{pmatrix} = \mathbf{A}^N \quad \text{and} \quad \begin{pmatrix} \alpha_{2i+1} & \alpha_{2i+2} \\ \beta_{2i+1} & \beta_{2i+2} \end{pmatrix} = \mathbf{A}^{N-i} \begin{pmatrix} \sqrt{1-t_a^2} & 0 \\ 0 & \sqrt{1-t_b^2} \end{pmatrix}.$$

Hence each of the  $N$  vacuum modes  $\hat{x}_i$  contribute a term to the variance in Eq. (10):

$$\begin{aligned}
(\alpha_1 \alpha_{2i+1} - \beta_1 \beta_{2i+1})^2 &= (\alpha_1, -\beta_1) \begin{pmatrix} \alpha_{2i+1} \\ \beta_{2i+1} \end{pmatrix} (\alpha_{2i+1}, \beta_{2i+1}) \begin{pmatrix} \alpha_1 \\ -\beta_1 \end{pmatrix} \\
&= (\alpha_1, -\beta_1) \mathbf{A}^{N-i} \begin{pmatrix} \sqrt{1-t_a^2} \\ 0 \end{pmatrix} (\sqrt{1-t_a^2}, 0) (\mathbf{A}^T)^{N-i} \begin{pmatrix} \alpha_1 \\ -\beta_1 \end{pmatrix} \\
&= (\alpha_1, -\beta_1) \mathbf{A}^{N-i} \begin{pmatrix} 1-t_a^2 & 0 \\ 0 & 0 \end{pmatrix} \mathbf{A}^{N-i} \begin{pmatrix} \alpha_1 \\ -\beta_1 \end{pmatrix}. \tag{11}
\end{aligned}$$

Each operator  $\hat{y}_i^\dagger$  contributes a term analogous to Eq. (11), but whose diagonal matrix is  $[0 \ 1 - t_b^2]$ . Temporarily neglecting the  $i = 1, 2$  contributions to the variance in Eq. (10), and summing over the vacuum contributions gives

$$\sum_{i>2} (\alpha_1 \alpha_i - \beta_1 \beta_i)^2 = (\alpha_1, -\beta_1) \left\{ \sum_{i=1}^N \mathbf{A}^{N-i} \begin{pmatrix} 1-t_a^2 & 0 \\ 0 & 1-t_b^2 \end{pmatrix} \mathbf{A}^{N-i} \right\} \begin{pmatrix} \alpha_1 \\ -\beta_1 \end{pmatrix}. \tag{12}$$

The continuum behaviour is recovered in the limit  $N \rightarrow \infty$ . To obtain a closed form expression for the sum, the infinitesimal parameters are expanded as a power series in  $1/N$ . Expanding the elements of  $\mathbf{A}$  in Eq. (8) gives

$$\mathbf{A} = 1 + \frac{1}{N} \mathbf{A}_0 + O\left(\frac{1}{N^2}\right) \quad \text{where} \quad \mathbf{A}_0 = \begin{pmatrix} \frac{1}{2} \log T_a & S \\ S & \frac{1}{2} \log T_b \end{pmatrix}. \tag{13}$$

Similarly taking  $t_a^2 = \exp(\frac{1}{N} \log T_a) \simeq 1 + \frac{1}{N} \log T_a$ , the sum in braces in Eq. (12) is

$$\mathbf{X} = \sum_{i=1}^N \mathbf{A}^{N-i} \left(\frac{1}{N} \mathbf{T}\right) \mathbf{A}^{N-i} = \frac{1}{N} \sum_{i=0}^{N-1} \mathbf{A}^i \mathbf{T} \mathbf{A}^i \quad \text{with} \quad \mathbf{T} = \begin{pmatrix} -\log T_a & 0 \\ 0 & -\log T_b \end{pmatrix}.$$

It can be easily verified that this sum obeys the geometric series relation

$$\mathbf{A} \mathbf{X} \mathbf{A} - \mathbf{X} = \frac{1}{N} (\mathbf{A}^N \mathbf{T} \mathbf{A}^N - \mathbf{T}).$$

Expanding to order  $1/N$  using Eq. (13) gives

$$\mathbf{A} \mathbf{X} \mathbf{A} - \mathbf{X} = \frac{1}{N} \{\mathbf{A}_0 \mathbf{X} + \mathbf{X} \mathbf{A}_0\} \Rightarrow \mathbf{A}_0 \mathbf{X} + \mathbf{X} \mathbf{A}_0 = \mathbf{A}^N \mathbf{T} \mathbf{A}^N - \mathbf{T}.$$

Taking the limit  $N \rightarrow \infty$ , the neglected  $O(1/N^2)$  terms vanish and  $\mathbf{A}^N \rightarrow \exp(\mathbf{A}_0)$ . Hence the sum  $\mathbf{X}$  converges and obeys

$$\mathbf{A}_0 \mathbf{X} + \mathbf{X} \mathbf{A}_0 = \exp(\mathbf{A}_0) \mathbf{T} \exp(\mathbf{A}_0) - \mathbf{T}. \tag{14}$$

This is a system of four linear equations for the elements of  $\mathbf{X}$  in terms of the model parameters  $T_a, T_b$  and  $S$ , and can be solved algebraically.

The sum  $\mathbf{X}$  contains all terms in the variance of Eq. (10) except  $i = 1, 2$  which correspond to the probe and conjugate coefficients. The probe contribution is

$$(\alpha_1^2 - \beta_1^2)^2 = \left\{ (\alpha_1, -\beta_1) \begin{pmatrix} \alpha_1 \\ \beta_1 \end{pmatrix} \right\}^2 = (\alpha_1, -\beta_1) e^{\mathbf{A}_0} \begin{pmatrix} 1 & 0 \\ 0 & 0 \end{pmatrix} e^{\mathbf{A}_0} \begin{pmatrix} \alpha_1 \\ -\beta_1 \end{pmatrix},$$

while the conjugate contribution  $(\alpha_1 \alpha_2 - \beta_1 \beta_2)^2$  has diagonal  $[0 \ 1]$ . Computing the full variance sum in Eq. (10) yields

$$\text{Var}(\hat{N}_a - \hat{N}_b) = (\alpha_1, -\beta_1) \left\{ e^{2\mathbf{A}_0} + \mathbf{X} \right\} \begin{pmatrix} \alpha_1 \\ -\beta_1 \end{pmatrix} \quad \text{with} \quad \begin{pmatrix} \alpha_1 \\ -\beta_1 \end{pmatrix} = \begin{pmatrix} 1 & 0 \\ 0 & -1 \end{pmatrix} e^{\mathbf{A}_0} \begin{pmatrix} 1 \\ 0 \end{pmatrix}.$$

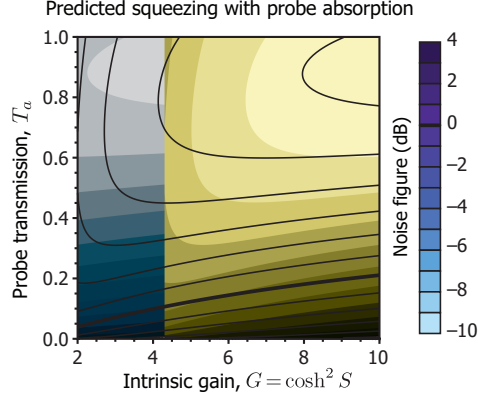


Fig. 3. Predicted squeezing for four-wave mixing with negligible conjugate absorption and net detection efficiency  $\eta = 85\%$ .

We introduce one final stage of loss to model optical losses after mixing (as in §4), scaling each coefficient by the relevant transmission factor ( $\sqrt{\eta_a}$  or  $\sqrt{\eta_b}$ ) and introducing the extra vacuum contributions  $\eta_a(1 - \eta_a)\alpha_1^2 + \eta_b(1 - \eta_b)\beta_1^2$ . The net variance in Eq. (10) is therefore

$$\text{Var}(\hat{N}_a - \hat{N}_b) = (\alpha_1, -\beta_1) \left\{ \mathbf{P}(e^{2\mathbf{A}_0} + \mathbf{X})\mathbf{P} + (1 - \mathbf{P})\mathbf{P} \right\} \begin{pmatrix} \alpha_1 \\ -\beta_1 \end{pmatrix} \langle \hat{N}_0 \rangle \text{ where } \mathbf{P} = \begin{pmatrix} \eta_a & 0 \\ 0 & \eta_b \end{pmatrix}.$$

The measured beam powers relative to the incident probe power (the “effective gains”) are

$$G_a \equiv \frac{\langle \hat{N}_a \rangle}{\langle \hat{N}_0 \rangle} = \eta_a \alpha_1^2 \quad \text{and} \quad G_b \equiv \frac{\langle \hat{N}_b \rangle}{\langle \hat{N}_0 \rangle} = \eta_b \alpha_2^2 \quad \text{with} \quad \begin{pmatrix} \alpha_1 \\ \alpha_2 \end{pmatrix} = e^{\mathbf{A}_0} \begin{pmatrix} 1 \\ 0 \end{pmatrix}, \quad (15)$$

and the relevant shot-noise limit is  $\text{Var}(\hat{N}_a - \hat{N}_b)_{\text{SNL}} = \langle N_a \rangle + \langle N_b \rangle = (\eta_a \alpha_1^2 + \eta_b \beta_1^2) \langle \hat{N}_0 \rangle$ .

Evaluating all the contributions to Eq. (10), we obtain an analytic expression for the degree of relative intensity squeezing produced by this system. This expression is algebraic in  $T_a$ ,  $T_b$  and  $S$ , but runs to a dozen typeset lines. However, special cases are readily derived and provide physical insight not readily accessible from numerical models.

In the experimentally studied case (Refs. [1–7]), detection efficiencies are carefully balanced ( $\eta_a = \eta_b \equiv \eta$ ) and the far-detuned conjugate experiences negligible absorption ( $T_b = 1$ ). The corresponding degree of squeezing is

$$\text{NF} = 1 - \eta \frac{2S \sinh^2 \xi}{\xi \cosh(2\xi + \chi)} + \eta \sqrt{T_a} \frac{S \log^2 T_a \sinh^4 \xi}{2\xi^3 \cosh(2\xi + \chi)}, \quad (16)$$

with parameters  $\xi = \frac{1}{4} \sqrt{16S^2 + (\log T_a - \log T_b)^2}$  and  $\tanh \chi = (\log T_a - \log T_b) / 4\xi$ . The three terms describe the shot-noise limit, correlations from four-wave mixing, and injected vacuum noise.

Figure 3 shows the noise figure as a function of the probe transmission  $T_a$  and intrinsic mixing gain  $G = \cosh^2 S$  (in excellent agreement with the numerical model of Ref. [3]). Note the counter-intuitive result that the strongest squeezing is obtained with imperfect transmission ( $T_a < 1$ ). This is because the shot noise carried by the incident probe beam is also amplified by the mixing process, and a small “optimal” level of probe loss decreases this contribution to the measured noise power before injected vacuum noise dominates. This optimal level is easily obtained by minimizing Eq. (16).

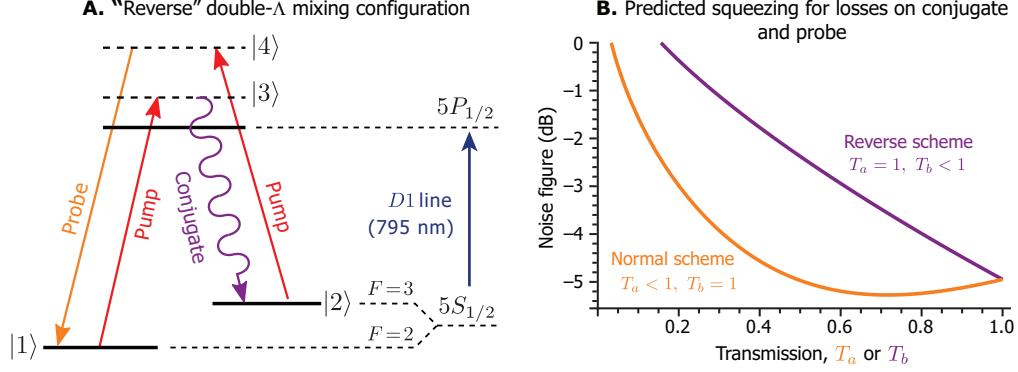


Fig. 4. (A) Four-wave mixing in the “reverse” configuration. (B) Predicted squeezing for four-wave mixing in the normal/reverse configurations with intrinsic gain  $G = 3$ .

The model can also be applied to other four-wave mixing systems. For example, interchanging the probe and conjugate wavelengths produces the “reverse” configuration (Fig. 4A). This system is interesting as the weakly-coupled conjugate transition is brought closer to resonance, producing much higher intrinsic mixing gain for the same beam powers. In this case, the probe experiences negligible absorption ( $T_a = 1$ ) compared to the conjugate ( $T_b < 1$ ), and the predicted squeezing is

$$\text{NF} = 1 - \eta \frac{2S \cosh^2(\xi + \chi)}{\xi \cosh(2\xi + \chi)} + \eta \sqrt{T_b} \frac{S(4S - \log T_b \sinh(2\xi + \chi))^2}{8\xi^3 \cosh(2\xi + \chi)}. \quad (17)$$

The vacuum noise term in Eq. (17) is considerably larger than in Eq. (16), resulting in several decibels difference for moderate levels of absorption (Fig. 4B). Unlike the probe losses discussed above, losses on the conjugate only destroy correlations and introduce noise, so squeezing by four-wave mixing in the reverse configuration is always less effective for the same level of intrinsic mixing gain.

Finally, it is worth noting for consistency that in the limit of both  $T_a, T_b \rightarrow 1$ , the post-mixing optical-loss result of Eq. (5) is obtained.

## 5. Experimental diagnostic

The analytic model derived above provides a simple yet powerful tool for optimizing the degree of squeezing obtained experimentally. It not only predicts which parameters will provide optimal results, but can also be used as a diagnostic tool to determine which factors are limiting the experimentally measured degree of squeezing.

To demonstrate this, we constructed a four-wave mixing apparatus as described in Ref. [1]. A 400 mW pump beam intersects a 100  $\mu$ W probe beam with  $1/e^2$  beam waists of 630  $\mu$ m and 375  $\mu$ m respectively at an angle of 0.3° within a pure  $^{85}\text{Rb}$  vapor cell of internal length 7 mm heated to 130°C (Fig. 1B). The probe was generated by an AOM with fixed detuning 3040 MHz below the pump, which was scanned across the Doppler broadened  $D_1$  resonance at 795 nm. The relative intensity between probe and conjugate was measured with a balanced photodetector (Thorlabs PDB150A), refitted with high-efficiency photodiodes (Hamamatsu S3883, net efficiency 95%). The overall detection efficiency of the system was  $\eta = 85 \pm 1\%$ . The relative intensity noise was measured with a Rhode & Schwarz FSP7 spectrum analyzer at an analysis frequency of 1 MHz with 30 kHz resolution bandwidth.

The effective probe and conjugate gains ( $G_a$  and  $G_b$ ) were measured as a function of pump



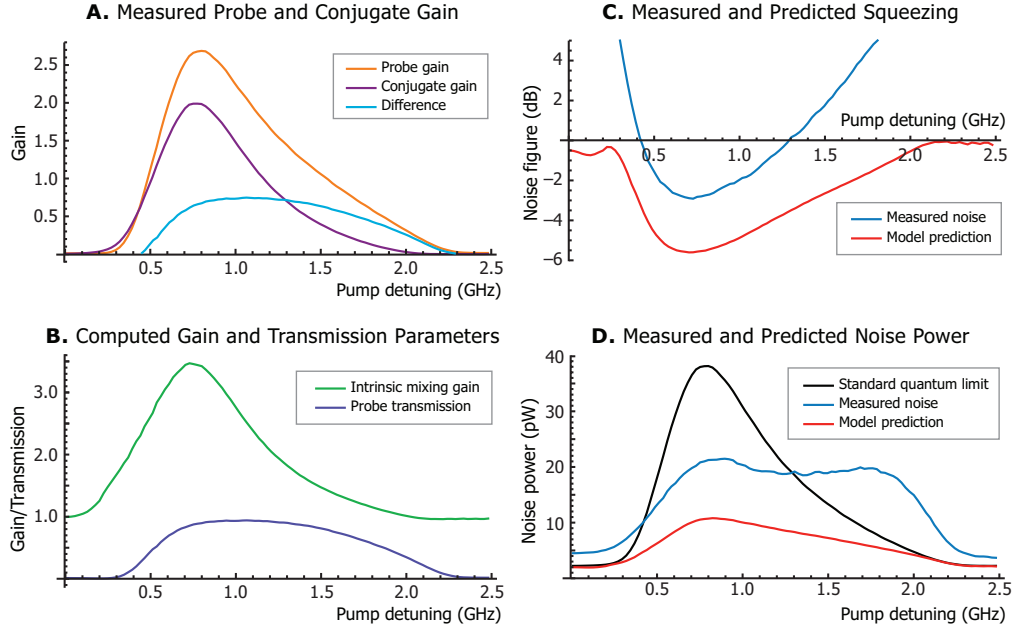


Fig. 5. (A) Measured probe and conjugate gain across four-wave mixing resonance and (B) inferred model parameters. (C) Experimentally measured squeezing and (D) associated noise powers compared to model predictions for these parameters. Detunings are for pump beam and are measured above the centre of the  $^{85}\text{Rb } 5S_{1/2}(F=2) \rightarrow 5P_{1/2}$  transition.

beam detuning (Fig. 5A) and used to simultaneously solve Eq. (15) for the intrinsic gain  $G$  and probe transmission  $T_a$  (Fig. 5B) via the coefficients  $\alpha_1$  and  $\alpha_2$ . Note that the gain resonance extends well into the Doppler-broadened absorption resonance for detunings below 600 MHz from the line-centre, demonstrating strong competition between the processes.

The model predicts significantly stronger squeezing should be possible for these parameters than measured experimentally (Fig. 5C). As our incident probe beam was measured to be shot-noise limited, this demonstrates that our noise measurement was limited by technical factors and not by insufficient intrinsic gain or excessive absorption.

One cause for our discrepancy is the technical difficulty in eliminating the bright pump beam after the vapor cell. Detection of the pump introduces uncorrelated fluctuations and increases the measured noise level [3]. This is evident around zero detuning, where the probe is fully absorbed (Fig. 5A) but the measured noise is far above the standard quantum limit (Fig. 5D). Upon blocking the pump beam, the relative intensity noise was measured at the shot-noise limit. Subtracting this background level implies that  $-4.1$  dB of squeezing would be obtained by eliminating cross-beam detection.

The model assumes that gain occurs uniformly throughout the vapor cell, which requires that the beams be overlapped over the entire region. If the beams are not properly overlapped, the mixing strength decreases and gain becomes spatially varying. As losses are unchanged, the relative intensity noise increases as a result. This is likely the cause of the remaining discrepancy, and improved squeezing could be achieved by manipulating beam alignment and waists to ensure proper overlap throughout the cell.

## 6. Conclusions

We have presented a method for analytically calculating the degree of squeezing produced by a four-wave mixing system in the presence of absorption. Our model included the contributions from arbitrarily many injected vacuum modes that were subsequently squeezed by the system, producing an ab-initio quantum mechanical description of the introduced losses. Our general result is not reliant on implementation details and can be applied to analyze any four-wave mixing scheme, while the matrix methods techniques we developed can be applied to model other systems both within quantum optics and more generally.

We considered two special cases, corresponding to the experimentally studied system (introduced in Ref. [1]) and the “reverse” configuration, with probe and conjugate wavelengths interchanged. We presented closed-form expressions for the relative intensity noise in these cases, and demonstrated that a small level of probe loss was desirable to suppress amplification of the initial shot-noise. The reverse configuration was shown to produce the same squeezing at equal gain for ideal transmission, but was significantly more sensitive to losses.

The model was applied to analyze experimentally measured squeezing and determine the intrinsic mixing gain and transmission factors of the four-wave mixing resonance. Comparing the expected squeezing to measured results provided insight into the factors limiting our measurement and hence where to direct effort in optimizing the many free parameters of the system.

While it should be noted that this model considers the propagation of a Gaussian beam mode only, an arbitrary beam can be analyzed as a product state of orthogonal spatial modes, with each mode independently squeezed [4]. The model established in this paper may therefore be applied to each pair of spatial modes and the resulting noise powers summed to obtain the overall relative intensity squeezing for a multi-mode beam. Such multi-mode squeezing has been experimentally demonstrated [5], with promising applications in quantum imaging.